Design of Surface Plasmon Resonance Devices for Biosensing

Author: Kamran Latif Akhtar.
Advisor: Mauricio Moreno Sereno
Facultat de Física, Universitat de Barcelona, Diagonal 645, 08028 Barcelona, Spain.*

Abstract: A study of the effects of geometry of a SPR device based on a gold nanohole array for its use as a biosensor has been done. For this, the OptiFDTD software has been used. It has allowed to obtain the dependence between the position of the SPR dip and the period, the diameter of the hole and the thickness of the gold film. The simulations have been done for mediums with different refractive index to observe the effect of using different substances. Small shifts in the SPR peak have been observed caused by little changes in the refractive index. The results obtained are the expected ones, as there are many biosensing devices based on this principle.

I. INTRODUCTION

Surface plasmon resonance (SPR) consists of the collective resonance of conduction electrons due to stimulation by light. This oscillation of electrons takes place at the interface between negative and positive permittivity materials, that is, between a metal and a dielectric material.

When transverse magnetic (TM) p-polarized light strikes on the interface, a dip in the intensity of the reflected light can be observed due to the resonance effect, at a certain angle, caused by the interaction between the incident TM light and some of the free electrons of the metal layer, that start oscillating.

On a flat surface, no optical coupling is allowed because the surface plasmon (SP) has a greater momentum than an optical field traversing above the surface. [1]

SPR can be observed through various techniques, such as the Kretschmann configuration, which is used most in practical applications. In the Kretschmann configuration, a thin metal film, such as gold, is often evaporated on the surface of a triangular or semi-circular prism. This is not always the case, if we want to reuse the prism, gold is then evaporated on a plane substrate and an index adapting liquid is placed between the base of the prism and the substrate. Then, the block is illuminated at a specific angle which causes an evanescent wave to penetrate through the metal film, causing plasmons to be excited at the outer side of the gold film.

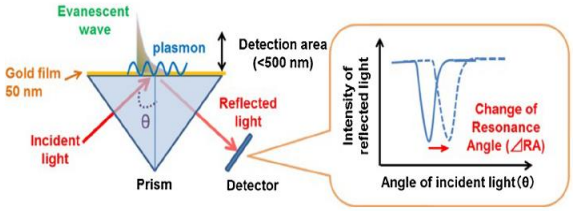

FIGURE 1: SPR system using Kretschmann configuration and figure of the intensity of reflected light as a function of the angle of incidence as measured by the detector.

However, on a patterned surface, as we can observe in Figure 2, the optical field can scatter to states with a higher momentum and excite a surface plasmon polariton (SPP), which is an optically active mixture of surface plasmon and optical fields.

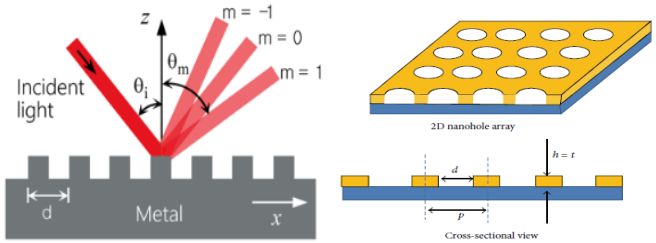

FIGURE 2: On the left, light diffraction by 1D grating, where m represents the diffraction order and θ_m the diffraction angle, one of which excites a plasmon. On the right, 2D square nanohole plasmonic substrate. Varying parameters such as layer thickness, hole diameter and period we can obtain different sensitivities. [2]

The sensitivity of the device can be tuned by changing the periodicity of the structure, the size of the hole, the thickness of the thin metal film and the shape of the structure. Highly sensitive sensors have been developed using these configurations for their use in varied applications such as biological and chemical sensing, gas sensing and clinical diagnostics. [3]

An alternative to the angular configuration, in which we vary the incidence angle at a fixed wavelength, is the spectral mode, in which we vary the wavelength at a fixed angle. In this case we will observe resonance in the reflectance spectrum for a narrow wavelength band, due to the fulfilment of the resonance conditions by the oscillating electrons. This is applicable both for nanostructured surfaces and prisms.

Subwavelength gratings can be created to reflect a narrow band of wavelengths and produce a sharp peak in the reflection spectrum. The resonance wavelength is determined by the period of the grating and the effective refractive index under resonance conditions:

$$\lambda_{resonance} = n_{eff}\,\Lambda \qquad (1)$$

II. APPLICATIONS FOR BIOSENSORS

Sensitive technologies, such as surface plasmon resonance and photonic crystal (PC) based biosensors have been used as diagnostic devices. These biosensors hold many advantages such as cost-effective fabrication and short assay time. They

* Electronic address: kam.latif23@gmail.com

have been used to detect a wide array of biotargets, proteins, nucleic acids, pathogens and cancer biomarkers. [4]

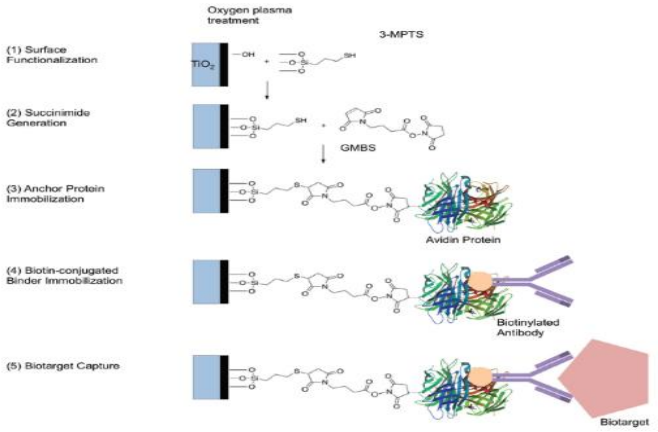

FIGURE 3: Surface chemistry approach used for capturing biotargets for biosensing purposes.

To ensure the capture of the biotarget, surface chemistry approaches are used. These consist of an active layer that immobilizes binder molecules. Depending on the material, different functionalization strategies are used, such as physical adsorption (via hydrogen bonds and Van der Waals interactions) and covalent binding (using the strong chemical linkage between a surface and binder molecules).

A biochemical interaction on the surface causes a change in the effective refractive index, which results in a shift of the resonance wavelength peak, which is proportional to the concentration of the biotarget, as we can observe in Figure 3.

III. SPR DESIGN AND FABRICATION

There are a number of periodic structure designs that can be used for this particular experiment. Next, we are going to describe one, nanohole fabrication process by thermal nano-imprint lithography.

The nanohole array fabrication process in this case is the following, as shown in Figure 4. The nanohole array is obtained with stamps fabricated by thermal nano-imprint lithography, residual layer etching and Ti/Au deposition and lift-off processes.

A 10cm thick glass wafer is used to carry out the imprinting process and is coated with a 100nm thermoplastic polymer layer. To obtain this layer, we need to spin coat it at 3000rpm for 30s. The nanoimprint lithography is carried out in a hot-embossing system. Afterwards the residual layer is etched by O_2 plasma.

With this process, the polymer is etched homogeneously until the residual layer has been fully removed and the pattern has been conveyed onto the substrate. Electron beam evaporation is used to deposit a metallic Ti (adhesion layer, 5nm) /Au (50nm) layer. Lastly, the resist lift-off process to obtain the nanohole array structure is carried out in an ultrasonic hot acetone bath. [5]

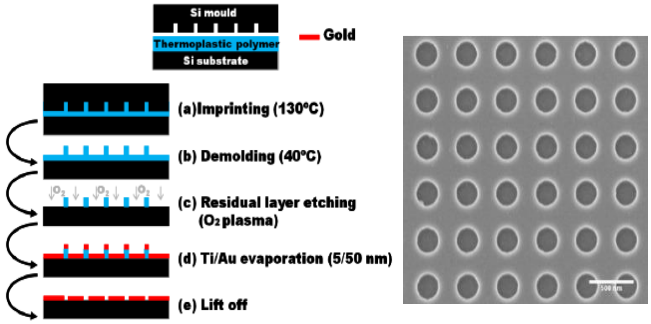

FIGURE 4: Nanohole fabrication process and SEM image of a gold nanohole array with a 250nm hole diameter and a periodicity of 450nm.

IV. SIMULATION SOFTWARE

OptiFDTD 64-bit software was used to design and analyse the SPR structures. It takes propagation, scattering, reflection, diffraction, polarization and nonlinear phenomena into account.

It is based on the FDTD (Finite-Difference Time-Domain) method, which solves Maxwell equations in a numerical grid, with second order numerical accuracy. The algorithm solves both electric and magnetic fields in spatial and temporal domains, using the full-vector differential form of Maxwell's coupled curl equations. [6]

$$\nabla \times \vec{E} = -\mu \frac{\partial \vec{H}}{\partial t} \qquad (2)$$

$$\nabla \times \vec{H} = \varepsilon \frac{\partial \vec{E}}{\partial t} + \sigma \vec{E} \qquad (3)$$

Applying the second order finite difference method to equations (2) and (3), 3D FDTD equations can be built, the domain of which is a cubic box, known as a Yee lattice, that contains the three components of $\vec{E}$ stored on edges of the cube, while the components of $\vec{H}$ are stored on the cubes faces. [7] The purpose of this study is to analyse the reflection spectrum of the SPR system, which consists of a SiO_2 substrate, a thin 5nm titanium layer below a thin gold layer with a cylindric hole of a certain diameter. The titanium layer is used so it and the gold layer form a metal alloy in order to get good adhesion to the substrate.

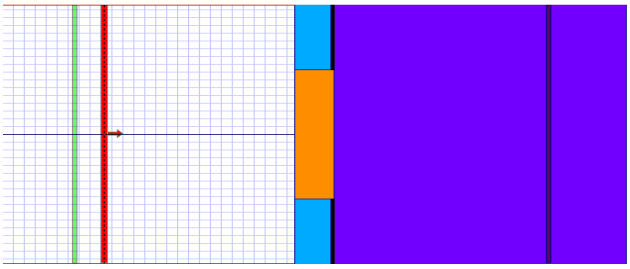

FIGURE 5: Simulated design in OPTIFDTD designer. The purple material corresponds to the SiO_2 substrate, the black material to the Titanium, the blue one to Gold and the orange corresponds to the hole.

In Figure 5 we can see both the transmission detector, in the substrate and the reflection detector, in green on the left. An input plane wave (in red in Figure 5) modulated as a Gaussian Continuous Wave with a central wavelength of 700nm was used, the width of which is controlled by the half width parameter. The sample is illuminated along the z axis and detectors are placed to visualize the reflection and transmission spectra.

In the studied cases we used periodic boundary conditions (PBC) in the x and y axis as only one individual cell was simulated at a time, to reduce computational costs. Anisotropic perfect match layers (APML) approach was used in the z axis.

V. SIMULATIONS AND RESULTS

All the simulations were conducted with the same simulation parameters: sampling mesh Δx=0.005μm, Δy=0.005μm, Δz=0.005μm, running for 12.000 time steps.

For these parameters and the geometry in Figure 5, we simulated the spectrum, changing some key parameters to observe the response and the sensitivity of the device.

The position of the reflectance dip is a function of the period of the structure, the diameter of the hole and the thickness of the gold layer. Furthermore, if we change the refraction index of the medium, we will also observe a displacement of the dip, which can give us information about the sensitivity for each case of study.

As external mediums for the study we used water (n=1.33), a material with a refraction index of n=1.35 to bridge the gap between water and PBS, PBS (n=1.37) and isopropanol (n=1.38). Mediums like air (n=1) or glycerol (n=1.48) weren't considered for this study as their resonance dips didn't fall inside the studied wavelength range. In order to study these two mediums, we would need to study a broader wavelength spectrum.

1. Sensitivity with different periods

First of all, simulations varying the period were conducted in order to know how it affects the reflectance, both the position and the depth of the dip.

Simulations were made both with and without a 5nm titanium layer below the gold layer.

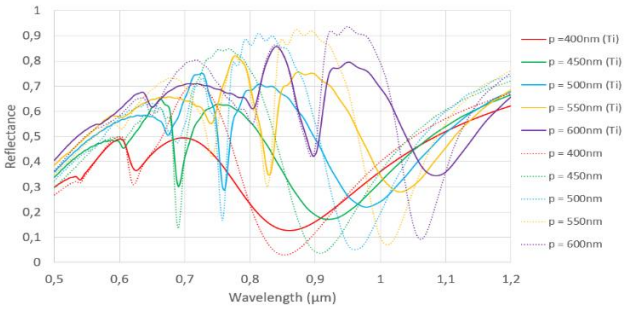

FIGURE 6: Reflection curves for the square nanohole array for different periods. The diameter of the hole is 250nm, the thickness of the gold film is 50nm and the external medium is water (n=1.33). The continuous lines correspond to simulations with a 5nm Titanium film, the spotted lines correspond to simulations without the Titanium film.

We can observe that the dips in reflectance are deeper when there is no titanium in the structure, however, from now on in this study all the structures will have the 5nm titanium layer in order to prevent fabrication issues. (see FIG 6)

From the information we get from the reflection curves, we can obtain the displacement of the SPR peak due to the change in the period, analysed both for the primary and the secondary dip.

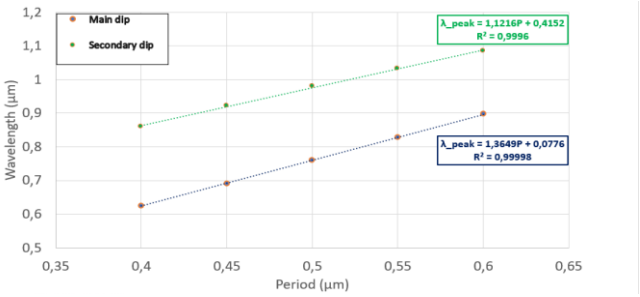

FIGURE 7: Position of the peak in the reflection spectra as a function of the period of the structure, for both the main dip and the secondary dip, with water as the external medium.

The displacement of the peak due to the change in period is linear, both for the main and the secondary dip, the wavelength of the SPR peak increases with the period. (see FIG 7)

Next, we evaluate the sensitivity of the device by studying the displacement of the main dip for a certain periodicity, for the four different substances.

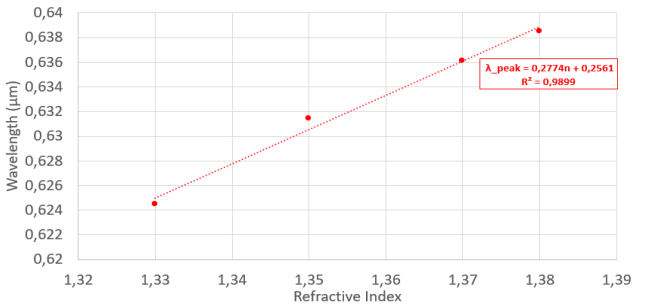

FIGURE 8: Dependence between the wavelength of the main SPR dip and the refractive index, for a period of 400nm.

The sensitivity corresponds to the slope of the regression which represents the change in the SPR resonant wavelength with the refractive index at a constant period, gold layer thickness and hole diameter. We can observe there's a linear dependence between the wavelength of the main dip and the refractive index. (see FIG 8)

Duty cycle	Period (nm)	Sensitivity
0.307	400	0.277
0.242	450	0.231
0.196	500	0.198
0.162	550	0.235
0.136	600	0.202

TABLE 1: Sensitivity of the device for the different duty cycles, varying the period. The duty cycle has been calculated as the fraction of the surface of a cell occupied by the hole. As we increase the period, maintaining the hole size constant, the duty cycle decreases.

As we can see in Table 1, the sensitivity of the device varies with the period of the structure. Periods between 400 and 600 nm have been studied.

Its highest value of 0.277 comes for a period of 400nm, although this might be due to the difficulty to determine properly the position of the SPR peak because of the width and little definition it has for all substances. Taking this effect into account, we can determine that the best sensitivity for the device comes for a period between 450-550nm which have a sensitivity of 0.231 and 0.235 respectively. For a period of 600nm we can see that the sensitivity starts to decrease and has a value of 0.202.

2. Sensitivity with different hole diameters

In second place, the dependence of the SPR resonance peak with the wavelength, alongside the sensitivity, were studied for different hole diameters.

Simulations for hole diameters between 200 and 300nm were conducted for the study. We can observe in Figure 9 that the size of the hole makes the resonance dip shift vertically, being the depth of the decay in reflectance similar in all hole sizes, but for smaller hole sizes the values of reflectance before and after the dip are higher.

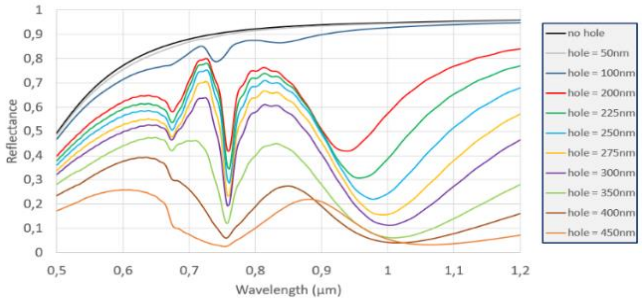

FIGURE 9: Reflection curves for different hole diameters. The period of the array is 500nm, the thickness of the gold film is 50nm and the external medium is water (n=1.33).

We can observe that hole size doesn't make the resonance wavelength change much for the main dip but it does for the secondary, wider dip.

Additionally, simulations for smaller holes were carried out in order to see that, if the hole is too small, we progressively lose definition and, in the end, in a surface with no hole, we find no resonance peak. On the other hand, if the hole is too large, relative to the size of the cell, we cease to observe the SPR resonance. (see FIG 9)

If we have a look at how the resonant wavelength changes with the hole diameter for both the main and secondary dips, we see that the shift is really small for the main dip and has a linear dependence for the wider, secondary dip. (see FIG 10).

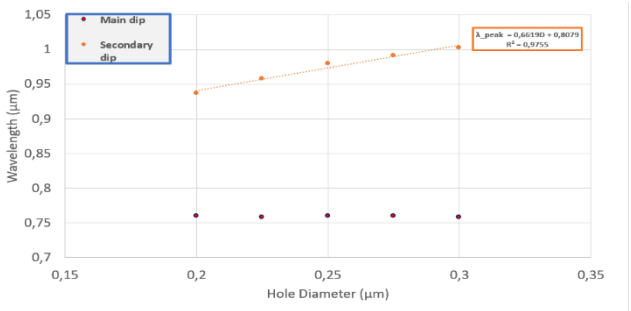

FIGURE 10: Resonance wavelengths as a function of the hole diameter for both dips. The period of the array is 500nm, the thickness of the gold film is 50nm and the external medium is water (n=1.33).

The main dip's position doesn't change much with the diameter of the hole, whereas it does for the secondary dip. We could use the main dip as a reference that doesn't change with the size of the hole and study the movement of the secondary dip, however, the secondary dip is too wide and would cause trouble when it comes to determining its displacement due to small refractive index changes.

Next, we simulate the different hole diameters for the 4 substances used as the external medium, for the main dip.

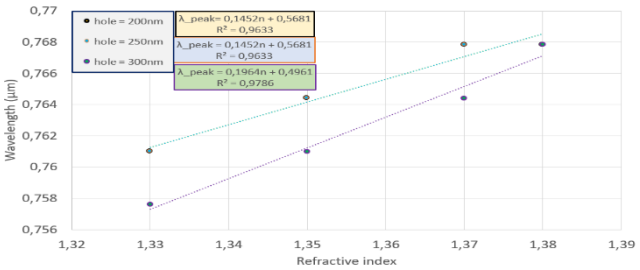

FIGURE 11: Resonance wavelengths as a function of the refractive index. The period of the array is 500nm and the thickness of the gold film is 50nm. Three different hole sizes are represented: 200nm (0.126 DC), 250nm (0.196 DC) and 300nm (0.282 DC).

When we look at the resonant wavelength for different substances, we see that there's a complete overlap in the case of the 200nm and 250nm holes, the sensitivity doesn't change much at all in this range, it has a value of 0.1452, this might be due to the fact that the shift of the peak is so small. Whereas if we have a look at the 300nm diameter hole, we see that its sensitivity is higher, with a value of 0.1964. (see FIG 11)

So, we can conclude that a change in the diameter of the hole induces a very small displacement of the resonant wavelength, while for larger holes we obtain a higher sensitivity.

3. Sensitivity with different gold film thickness

In this section we are going to study the effects that changing the gold film thickness has on our SPR device. Until now we've used a 50nm thick film, now we're going to vary this value between 20nm and 50nm.

First, we obtain the reflectance spectrum for the different film thicknesses.

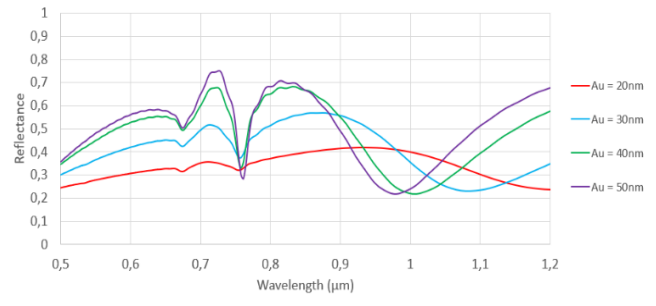

FIGURE 12: Reflection curves for gold film thicknesses. The period of the array is 500nm, the hole diameter is 250nm and the external medium is water (n=1.33).

We can see a clear dip for 40nm and 50nm thick gold film layers but for thinner films there is little to no absorption. (see FIG 12)

If we have a look at the displacement of the dip with wavelength, we'll see that the changes are very small, however, the peak moves to longer wavelengths when we increase the thickness. (see FIG 13)

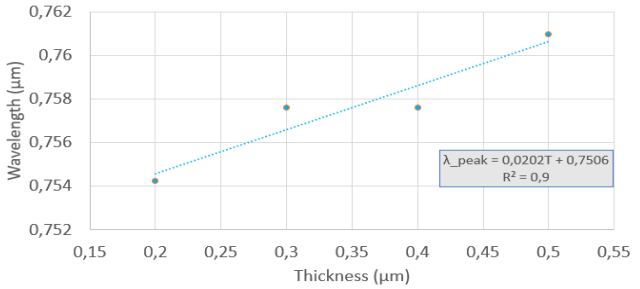

FIGURE 13: Resonance wavelengths as a function of the gold film thickness. The period of the array is 500nm, diameter of the hole is 250nm and the external medium is water (n=1.33).

Next, we carry out the simulations for the different substances to evaluate the dependence between sensitivity and gold film thickness.

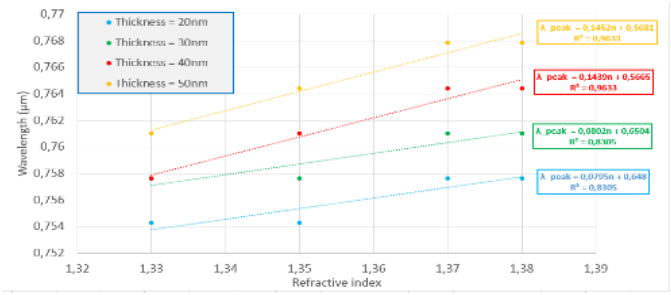

FIGURE 14: Resonance wavelengths as a function of the refractive index. The period of the array is 500nm, diameter of the hole is 250nm.

As we can observe, the resonant wavelength increases with the refractive index, linearly for thicker films and we can see as well that the thicker the film is, the more sensitive the SPR device becomes. (see FIG 14)

VI. CONCLUSIONS

- Working with 0.7µm light, increasing the period makes the SPR dip shift to infrared wavelengths. On the other hand, an increase to the hole diameter or the gold layer thickness doesn't alter the position of the dip significantly.
- By varying the period, we found that the highest sensitivity for this configuration comes in the range of 450-550nm. On the other hand, sensitivity increases with the diameter of the hole and the gold film thickness.
- The 5nm titanium layer used for adhesion of the gold film to the substrate affects the results by reducing the depth of the dips and by widening the secondary dip.
- An optimized configuration of the parameters of the experiment has been found, although the results show that sensitivity might increase if we increase the gold film thickness beyond the studied values, for instance.
- The SPR device works well in the context of biosensors as it can detect, as we've seen, small changes in the refractive index, that can prove useful, for example, when searching for the concentration of a certain biomarker or molecule.
- Δz=0.005µm was used as the z-mesh size in the simulations and it is the same as the thickness of the titanium layer (5nm). This might have led to not fully seeing the effect of the titanium layer. Simulations with a smaller mesh size in z would need to be carried out to see the effects, although this would increase simulation time significantly.

Acknowledgments

I would like to thank my advisor, Dr. Mauricio Moreno, for his help and tutoring during the entire project and for introducing me to research in applied physics.

I would also like to show gratitude for the help and support my family has provided me throughout this work.

[1] T. A. Kelf et al, «*Localized and delocalized plasmons in metallic nanovoids*» *Phys. Rev B 74,.245415 (*2006)

[2] Abid Ameen «*Ultra-Sensitive Colorimetric Plasmonic Sensing and Microfluidics for Biofluid Diagnostics Using Nanohole Array*» *Journal of Nanomaterials (2015)*

[3] Armin Agharazy Dormeny et al, *«Design and simulation of a refractive index sensor based on SPR and LSPR using gold nanostructures» Results in Physics 16 (2020)*

[4] Hakan Inan et al, *«Photonic crystals: emerging biosensors and their promise for point-of-care applications» Chem. Soc. Rev., (2017)*

[5] Josu Martinez-Perdiguero et al, «Real-Time Label-Free Surface Plasmon Resonance Biosensing with Gold Nanohole Arrays Fabricated by Nanoimprint Litography» *Sensors 13 (2013)*

[6] Optiwave documentation [online]: http://optiwave.com

[7] Meep documentation [online]: http://meep.readthedocs.io